ORIGINAL ARTICLE

Thomas Müller-Reichert · Ingrid Sassoon ·
Eileen O'Toole · Maryse Romao · Anthony J. Ashford ·
Anthony A. Hyman · Claude Antony

Analysis of the distribution of the kinetochore protein Ndc10p in *Saccharomyces cerevisiae* using 3-D modeling of mitotic spindles

Abstract Ndc10p is one of the DNA-binding constituents of the kinetochore in *Saccharomyces cerevisiae* but light microscopy analysis suggests that Ndc10p is not limited to kinetochore regions. We examined the localization of Ndc10p using immunoelectron microscopy and showed that Ndc10p is associated with spindle microtubules from S-phase through anaphase. By serial section reconstruction of mitotic spindles combined with immunogold detection, we showed that Ndc10p interacts with microtubules laterally as well as terminally. About 50% of the gold label in serial section reconstructions of short mitotic spindles was associated with the walls of spindle microtubules. Interaction of kinetochore components with microtubule walls was also shown for kinetochore protein Ndc80p. Our data suggest that at least a subset of kinetochore-associated protein is dispersed throughout the mitotic spindle.

Introduction

Kinetochores are protein complexes that bind to centromeric DNA to ensure the correct segregation of chromosomes at mitosis (reviewed by Nasmyth 2002). A

T. Müller-Reichert (✉) · A. J. Ashford · A. A. Hyman
Max Planck Institute of Molecular Cell Biology and Genetics,
Pfotenhauerstrasse 108, 01307 Dresden, Germany
e-mail: mueller-reichert@mpi-cbg.de

I. Sassoon
European Molecular Biology Laboratory,
Meyerhofstrasse 1, Postfach 10.2209, 69012 Heidelberg, Germany

E. O'Toole
Boulder Laboratory for 3-D Fine Structure,
Department of Molecular Cellular and Developmental Biology,
University of Colorado, Boulder, CO 80309-0347, USA

M. Romao · C. Antony
Institut Curie UMR144 CNRS,
26 rue d'Ulm, 75248 Paris cedex 05, France

mammalian centromere can be millions of base pairs in size, and this complexity has hindered the study of centromere function in animal cells (Cheeseman et al. 2002). The centromere of budding yeast, on the other hand, is only about 100 bp (Fitzgerald-Hayes et al. 1982). DNA recognition is carried out primarily at the CDE III element of the yeast centromere (reviewed by Hyman and Sorger 1995). CDEIII binds CBF3, an M_r 240,000 multiprotein complex consisting of Ndc10p, Cep3p, Ctf13p, and Skp1p (Lechner and Carbon 1991). CBF3 is an essential complex as its absence causes the loss of kinetochore function both in vivo and in vitro and the disruption of all interactions of kinetochore proteins with the centromere (Goh and Kilmartin 1993; Sorger et al. 1994; Ortiz et al. 1999). Apart from this complex, many other components play a role in kinetochore function (reviewed by Cheeseman et al. 2002). Recent reports have shown that Ndc80p in association with Spc24p, Spc25p and Nuf2p forms an evolutionarily conserved multiprotein complex, which is part of the central kinetochore and, like CBF3, essential for the correct segregation of chromosomes (Janke et al. 2001; Wigge and Kilmartin 2001). Other protein complexes are thought to have a "linking" function. For example, the Ctf19p complex (Ortiz et al. 1999) links CBF3 components to the Ctf3p (Measday et al. 2002) and the Ndc80p complex (Janke et al. 2001; Wigge and Kilmartin 2001). Finally, the Duo1p/Dam1p complex appears to be involved in both kinetochore function and spindle integrity (Cheeseman et al. 2001a, 2001b; Janke et al. 2002), and the Aurora kinase type Ipl1p, in a complex with Sli15p, is thought to control sister kinetochore orientation with respect to the poles (Tanaka et al. 2002).

Kinetochore complexes in mammalian cells are readily visible by light and electron microscopy upon their appearance after breakdown of the nuclear envelope, when chromatin is condensed (Roos 1973). In contrast, in *Saccharomyces cerevisiae*, kinetochores are not visible during mitosis (Peterson and Ris 1976; Winey et al. 1995) and the exact time course of their assembly is largely unknown. Although individual centromere loci in budding

yeast can be detected by light microscopy, using either in situ hybridization (Scherthan et al. 1992; Guacci et al. 1994) or expression of green fluorescent protein (GFP)-fusion proteins (Straight et al. 1997), the structure of the kinetochore complex in this organism could not be visualized even by electron microscopy. The aim of this study was to analyze the distribution of budding yeast kinetochores during mitosis by electron microscopy using Ndc10p as a primary target for immunolocalization. The *NDC10* gene has been isolated in a visual screen for abnormal spindle morphology (Goh and Kilmartin 1993; Jiang et al. 1993). The phenotype of *ndc10-1* cells at restrictive temperature is detachment of chromosomes from the spindle, while DNA replication, spindle formation, anaphase spindle elongation, and cytokinesis continue essentially normally (Goh and Kilmartin 1993). Another allele of *NDC10*, *ndc10-2*, exhibits anaphase spindles in which DNA is associated with only one pole (Sorger et al. 1995). In addition, localization of Mtw1p at the centromere is dependent on Ndc10p (Goshima and Yanagida 2000), and centromere clustering in the interphase nucleus is reduced by the *ndc10-1* mutation (Quanwen et al. 2000). In fact, the centromeric association of most if not all kinetochore proteins is dependent on Ndc10 protein (He et al. 2001). Therefore Ndc10p is considered as one of the core components of budding yeast kinetochores, and homologous proteins have not been described in either *Schizosaccharomyces pombe* or in mammalian systems. To date, Ndc10p has been localized by light microscopy to structures that resemble the entire mitotic spindle (Goh and Kilmartin 1993; Zeng et al. 1999; Goshima and Yanagida 2000). Interestingly, bilobed localization of kinetochore proteins on either side of the spindle midzone has been reported (Goshima and Yanagida 2000; He et al. 2000), and this pattern was related to the existence of transient sister chromatid separation. One possibility is that this distribution represents the sum of the distributions of all the kinetochores oscillating throughout the spindle. Because kinetochores are thought to bind to microtubule ends, we were therefore interested in determining the relationship between kinetochore localization and microtubule end interaction. By combining three-dimensional reconstruction of mitotic spindles with immunoelectron microscopy of the Ndc10p protein, we show that half of the detected antigens are associated terminally with the plus end of the spindle microtubules, while about half of the Ndc10p protein is clearly associated laterally with microtubule walls. Using an antibody against Ndc80p, we found that this kinetochore protein displays a similar pattern of distribution at the electron microscopy level.

Materials and methods

Yeast strains and growth conditions

The yeast strains and relevant genotypes used were as follows: THY658, *NDC10-GFP::TRP1* (this study); THY697, *Δcdc20::LEU2*, *GALCDC20::TRP1* (Lim et al. 1998). The background of all yeast strains is W303A. Green fluorescent protein tagging of Ndc10p was performed by the lithium acetate method (Ito et al. 1983) using a previously described *NDC10-GFP* fusion plasmid (Zeng et al. 1999). General molecular biology methods were carried out as described by Sambrook et al. (1989). Growth media including yeast extract/peptone/dextrose (YEPD) and yeast extract/peptone containing 2% raffinose and 2% galactose (YEPRG) were prepared as described (Rose et al. 1990). The wild-type strain expressing the Ndc10p-GFP fusion protein was grown in YEPD at 30°C. To obtain arrested metaphase spindles, *GALCDC20* cells were grown in YEPRG, centrifuged, and resuspended in YEPD. Cells were grown for 4 h at 30°C before harvesting.

Antibodies against kinetochore proteins

The plasmid pGEX-GST-NDC10 was kindly provided by J. Kilmartin (MRC, Cambridge, UK). It contains the C-terminal part of the *NDC10* gene (amino acids 679–894). It was transformed into BL21 bacteria and the glutathione (GST)-Ndc10p was renatured, purified over a GST column, and injected into rabbits. The sera obtained were subsequently purified over a GST-Ndc10p column and stored in 50% glycerol at −20°C (Sassoon et al. 1999). We also used polyclonal antibodies raised against Ndc10p, Ndc80p (Wigge et al. 1998) and Tub4p, the γ-tubulin of *S. cerevisiae* (all antibodies kindly provided by J. Kilmartin MRC, Cambridge, UK).

Immunofluorescence light microscopy

We performed indirect immunofluorescence on formaldehyde-fixed samples (Pringle et al. 1991; Hoyt et al. 1992). Kinetochore antigens were localized using the polyclonal GST-Ndc10p antibody and a previously described polyclonal antibody raised against Ndc80p. We labeled spindle microtubules using a monoclonal anti-α-tubulin antibody (Sigma; St. Louis, Mo.). Secondary antibodies for double labeling were a fluorescein-conjugated anti-rabbit antibody (1:200 dilution) and a rhodamine-conjugated anti-mouse antibody (1:200 dilution). All fluorescent conjugates were purchased from Sigma (St. Louis, Mo.). Yeast cells were examined with a Zeiss Axioskop epifluorescence microscope equipped with a 100× PlanApo oil immersion objective lens. Images were digitally captured using a Colour Cool View camera (Photonic Sciences, East Sussex). Image processing (i.e. background manipulation) was done using Adobe Photoshop (San José, Calif.).

Electron microscopy and immunocytochemistry

To preserve the ultrastructure of the spindle apparatus, yeast cells were high-pressure frozen as described (Ding et al. 1993; Winey et al. 1995; O'Toole et al. 1997; McDonald and Müller-Reichert 2002). Cells from mid-log phase cultures were harvested by vacuum filtration on 0.45 μm Millipore filters. After the cell paste had been transferred into specimen holders, samples were frozen using a BAL-TEC HPM 010 High Pressure Freezer (BAL-TEC, Liechtenstein). Freeze substitution of frozen cells was carried out in an automatic freeze substitution system (LEICA EM AFS; Leica, Vienna, Austria) for 3 days in 0.1% glutaraldehyde, 0.25% uranyl acetate, 0.01% OsO$_4$ in acetone at −90°C (Müller-Reichert et al. 2000). The freeze-substituted cells were gradually warmed to −50°C and embedded in Lowicryl resin (HM20). Polymerization of the resin was performed for 2 days each at −50°C and at 10°C. Thin sections (50–70 nm) were cut using a Reichert Ultracut Microtome (Leica, Vienna, Austria). The sections were collected on Formvar-coated nickel grids and processed for on-section immunolabeling.

For labeling of Ndc10p, we used the GST-Ndc10p antibody. In addition, we also tried to label Ndc10p-GFP using an affinity purified polyclonal antibody against GFP (raised by J. Kahana and P. Silver, Dana-Farber Cancer Institute, Boston, Mass.). Labeling

with the latter antibody was less efficient, possibly due to "masking" of the GFP tag in the fusion protein or the composition of the freeze-substitution cocktail. Using the same antibody against GFP, we tried to label Mtw1p-GFP and Cse4p-GFP on thin sections of wild-type cells (Goshima and Yanagida 2000). Due to either the masking effect or very low accessibility of antigens on the surface of the thin section, we could not obtain sufficient labeling signal (see discussion below). For labeling of another kinetochore component, we used the polyclonal antibody raised against Ndc80p (Wigge et al. 1998). The polyclonal antibody raised against Tub4p was used for a control experiment. All primary antibodies were diluted in blocking buffer containing 0.8% bovine serum albumin, 0.01% Tween 20, and 0.1% fish scale gelatin (Nycomed, Amersham) in PBS. The secondary goat anti-rabbit IgG antibody was coupled with 10 nm colloidal gold (British BioCell, UK). The antibody complex was stabilized by 1% glutaraldehyde in PBS. Immunolabeled sections were poststained with 2% uranyl acetate in 70% methanol for 4 min and Reynold's lead citrate for 2.5 min. Samples were imaged using a Philips CM120 (BioTWIN) (Eindhoven, The Netherlands) or a JEOL 100CX (Peabody, Mass., USA) electron microscope operated at 80 and 100 kV, respectively.

Serial section reconstruction and data analysis

For three-dimensional reconstructions, 50 nm serial sections of wild-type cells were imaged in a Philips CM10 electron microscope operated at 80 kV. The electron microscope was equipped with a rotating grid holder and a ±60° tilting stage. Rotating and tilting of the specimens allowed us to track microtubules in cross section from spindle pole body to spindle pole body. The tilt data were recorded for each image to correct for apparent section thickness. Images at 64,000× magnification were recorded by a CCD camera and transferred to a Silicon Graphics work station. Microtubule tracking, spindle alignment and stacking of the serial data were carried out as described (McDonald et al. 1991; Winey et al. 1995; O'Toole et al. 1997). We reconstructed four mitotic spindles of wild-type cells, ranging in length from 0.6 to 1.2 μm. In the three-dimensional wild-type models (two models are presented as stereo view pairs), microtubules were marked as follows: red and green lines represent microtubules originating from the opposite spindle pole bodies; blue lines, pole-to-pole microtubules. We also marked gold particles that represent immunolocalized Ndc10p with yellow dots, microtubule plus ends with blue dots, and microtubule plus ends associated with gold markers as pink dots. We determined the total number of gold particles bound, the total number of

microtubule plus ends, and the number of microtubule plus ends associated with gold labels. Using the largest reconstructed spindle (cell no. 1, 1.2 μm), we estimated the percentage of gold in the spindle that was associated with microtubule plus ends. For each gold particle, we determined the relative position on individual microtubules. We binned the data to generate a distribution plot. We also determined the percentage of gold-label antibodies in the wild-type nucleus that was associated with spindle microtubules. We counted the number of gold particles in the visible spindle area and the number of gold particles dispersed in the nucleus. To determine the position of Ndc10p in the arrested *GALCDC20* spindle, we searched our sections for cells whose spindle apparatus was oriented parallel to the plane of the section. We chose in preference those cells that showed the two spindle pole bodies. The spindle pole body close to the neck region of the duplicating cell was called "mother", the opposite spindle pole body was called "daughter" (Pereira et al. 2001). For each gold particle associated with the spindle, we measured its distance from the spindle pole bodies. We binned and normalized the data to show the distribution of Ndc10p between the two spindle pole bodies. As a control we mapped the position of Tub4p in the spindle using the same method.

Results

Ndc10p is associated with microtubules of forming, short and elongated spindles

Using an affinity-purified antibody that specifically recognizes recombinant as well as extracted wild-type Ndc10p on immunoblots (Fig. 1A) (Sassoon et al. 1999), we performed immunoelectron microscopy on cycling wild-type yeast cells (Fig. 1B). We found that the majority of the nuclear gold was associated with microtubules of the mitotic spindle (arrowheads). However, we also detected gold label dispersed in the yeast nucleus. We found no indication of specific labeling of components of the spindle pole body. Importantly, almost no labeling was observed at locations in the cytoplasm (c) or on cytoplasmic microtubules (arrows). About 80% of the
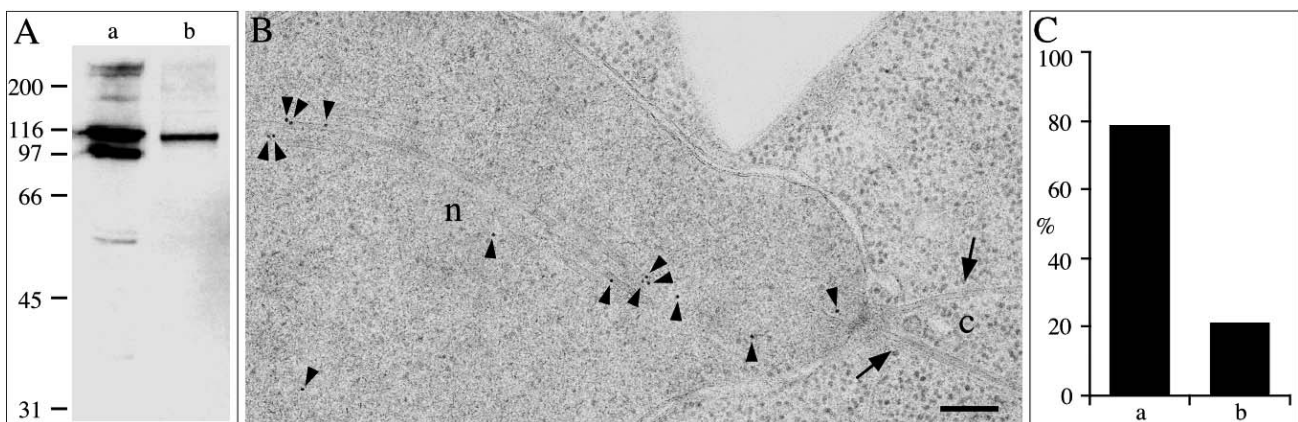
Fig. 1A–C Specificity of immunolabeling. **A** Immunoblot showing the detection of recombinant (*a*) and extracted wild-type Ndc10p (*b*). The antibody recognizes the full-size protein and degradation products of the baculovirus-expressed Ndc10p. **B** Immunoelectron microscopy showing the localization of Ndc10p in a wild-type cell. Gold labels (*arrowheads*) indicating Ndc10p were found predominantly associated with nuclear microtubules (*n*). Ndc10p could not be localized on cytoplasmic microtubules (*c*, *arrows*). **C** Quantitative analysis of immunolabeling. About 80% of the intranuclear signal was distributed in the spindle (*a*). Roughly, 20% of the colloidal gold was found dispersed in the nucleus (*b*). *Bar* represents 200 nm in **B**
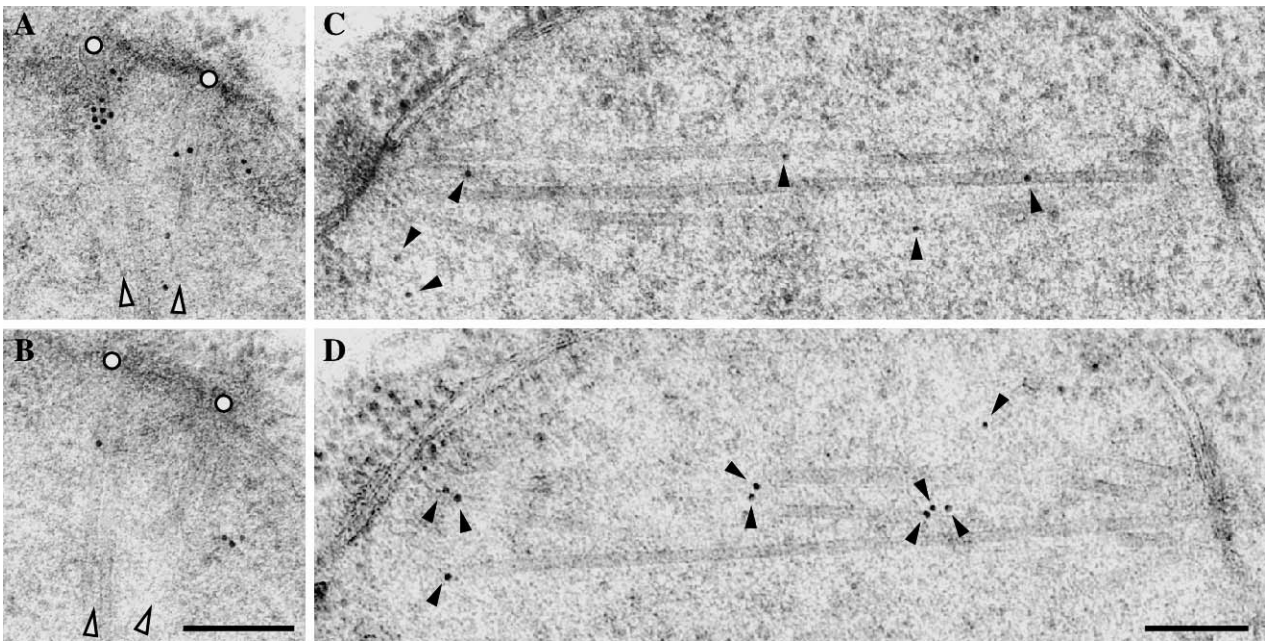
Fig. 2A–D Ultrastructural localization of Ndc10p in forming and short wild-type spindles. **A**, **B** Two serial sections of a forming spindle. The spindle pole bodies are marked by *open circles*, and the "direction" of the two half spindles is indicated by *arrowheads*. Labeling of Ndc10p was found on microtubules originating from both spindle poles. **C**, **D** Two serial, longitudinal sections of a short spindle. Ndc10p (*arrowheads*) is distributed in the spindle and appears to be associated with both short and long, pole-to-pole microtubules. Association of Ndc10p with the spindle pole bodies was not observed. *Bar* represents 200 nm in **B**, **D**

nuclear signal was distributed in the spindle (Fig. 1C, a), while 20% of the signal was dispersed (Fig. 1C, b).

Having shown that Ndc10p can be specifically recognized on Lowicryl sections prepared for immunoelectron microscopy, we followed the distribution of Ndc10p through the cell cycle. First, we examined the distribution of Ndc10p in S-phase. During S-phase, spindle pole bodies duplicate and microtubules grow out from the old and the new spindle pole body (Adams and Kilmartin 2000). Two serial sections of a forming spindle are shown in Fig. 2A, B. Open circles indicate the approximate centers of the two spindle pole bodies and arrows mark the " direction" of the microtubules. After duplication of the spindle pole body, gold labels were found associated with microtubules originating from both spindle pole bodies. Next, we examined short bipolar spindles in the wild-type nucleus. Two serial sections of a short mitotic spindle are shown in Fig. 2C, D. We found gold labels distributed throughout the short spindle (arrowheads). In these longitudinal sections, Ndc10p appears to be attached to both short and long pole-to-pole microtubules. In addition, Ndc10p appears to be associated with microtubule walls as well as with microtubule ends. Finally we examined long, anaphase spindles. An elongated spindle is schematized in Fig. 3A. The insert shows a half spindle ranging from the spindle pole body (spb) to the neck region (nr), as displayed in Fig. 3B, C. In accordance with light microscopic observations (Goh and Kilmartin 1993; Zeng et al. 1999; Goshima and Yanagida 2000), we found gold labeling close to the spindle pole bodies as well as along microtubules of anaphase spindles. Such a staining pattern was also observed in telophase-arrested *cdc15-2* cells (data not shown). From these data we conclude that gold is distributed throughout the length of the spindle microtubules.

Ndc10p is distributed homogenously
in metaphase-arrested spindles

To investigate the distribution of Ndc10p in short spindles, we labeled spindles arrested at metaphase by shut off of Cdc20p expression, which results in extremely synchronous mitotic arrest (Lim et al. 1998). After shifting the cells from galactose- to dextrose-containing growth medium, cells synchronously arrest with spindles of about 2.5 μm in length. For immunofluorescence light microscopy, we labeled Ndc10p in cycling and arrested *GALCDC20* cells (Fig. 4A). In control cultures growing in galactose, we found Ndc10p associated with microtubules of short and elongated spindles (white arrowheads), thus confirming the results obtained for wild-type spindles. After cell cycle arrest, we found intensive Ndc10p signal at the mitotic spindle. The spindle structure of an arrested *GALCDC20* cell as seen by electron microscopy is shown in Fig. 4B. The spindle has started to move into the bud region of the nucleus (black arrowheads). In this micrograph, both spindle pole bodies can be identified. We describe the spindle pole body most distant from the neck region as the daughter (d) and the spindle pole body closest to the neck region as the mother (m) (Pereira et al. 2001). We analyzed the distribution of
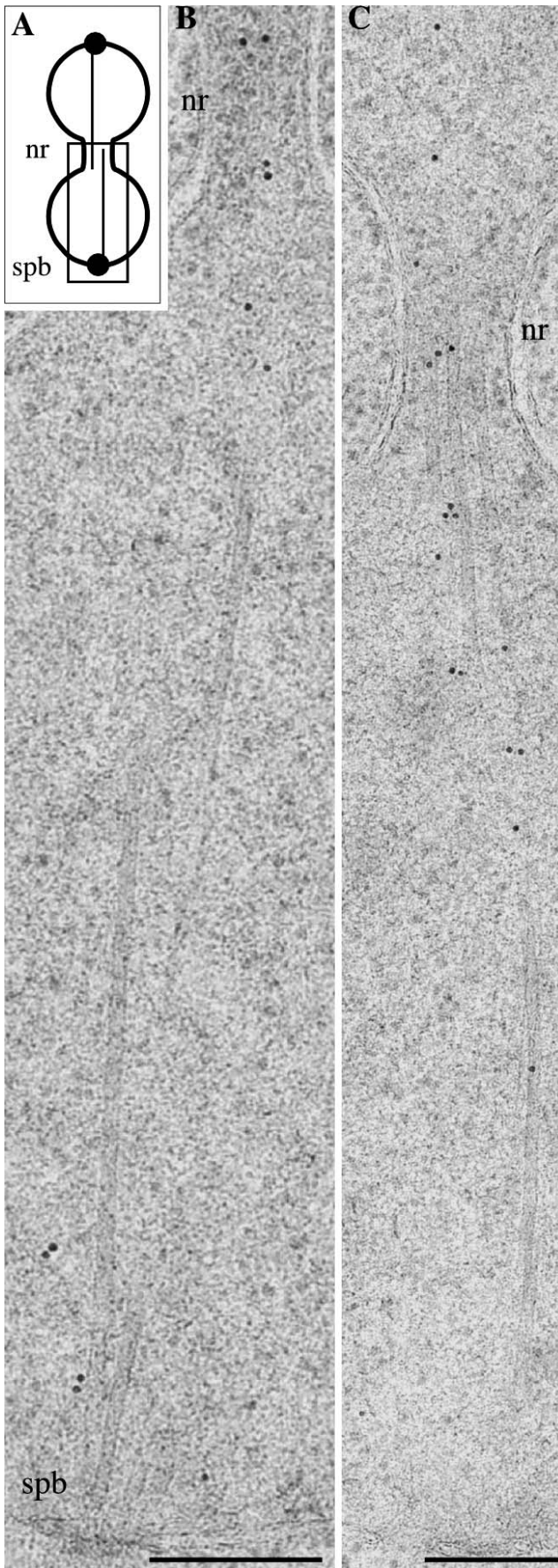
Ndc10p labels in longitudinal sections of arrested *GALCDC20* cells (Fig. 4C) and plotted the number of labels against the position in the spindle (Fig. 4D). The antigen is distributed homogenously in the arrested *GALCDC20* spindle. As a control, we also mapped the position of a γ-tubulin-like protein in the arrested spindle (Spang et al. 1996). An electron micrograph shows labeling of Tub4p at the daughter spindle pole body (Fig. 4E, arrow). Therefore, as for cycling cells, Ndc10p is homogeneously distributed along the spindle microtubules.

Ndc10p is laterally and terminally associated with microtubules

One main issue in this work was to determine whether Ndc10p is associated with the plus ends of spindle microtubules as expected for a conventional kinetochore location (Rieder and Alexander 1990; Skibbens et al. 1993). In mitotic spindles, Ndc10p appears to be associated with short as well as long interdigitating (i.e. pole-to-pole) microtubules. In addition, we found that Ndc10p appears to be attached to microtubules throughout their length in anaphase spindles. These observations suggest lateral as well as terminal association of Ndc10p with microtubules. An association with minus ends, however, is difficult to judge by viewing longitudinal thin sections through a spindle. Microtubule ends may be "hidden" in the thin section or artificially "created" during thin sectioning. To analyze the spatial relationship between microtubule plus ends and gold label more precisely, we used serial cross sections of labeled spindles to generate three-dimensional models (Fig. 5). We reconstructed four mitotic spindles of wild-type cells, ranging in length from 0.6–1.2 μm and therefore collected before the onset of anaphase. A three-dimensional model (stereo view) of a spindle of 1.2 μm length (cell no. 1) is shown in Fig. 5A, B. Microtubules originating from opposite spindle pole bodies are displayed in red and green. Microtubules that are continuous between the spindle pole bodies are shown in blue. Microtubule plus ends are marked with blue dots, and immunolabeling of Ndc10p is shown by yellow dots. Ndc10p labeling found at microtubule plus ends is marked by pink dots. Confirming our results shown in Fig. 1, we found that Ndc10p is associated with the spindle microtubules as well as spread throughout the nucleus. Because gold labels were found almost exclusively in the nucleus (see above), we interpret this dispersed signal to reflect endogenous, unbound Ndc10p.

Fig. 3A–C Localization of Ndc10p in longitudinal sections of wild-type, anaphase spindles. **A** Diagram of an elongated spindle. The *box* marks one half of the spindle from the spindle pole body (*spb*) to the neck region (*nr*) of the duplicated cell as displayed in **B** and **C**. In cells committed to anaphase, Ndc10p can be found along the length of the microtubules and is not localized predominantly in a region of the spindle close to the spindle pole body. *Bar* represents 250 nm in **B**, **C**
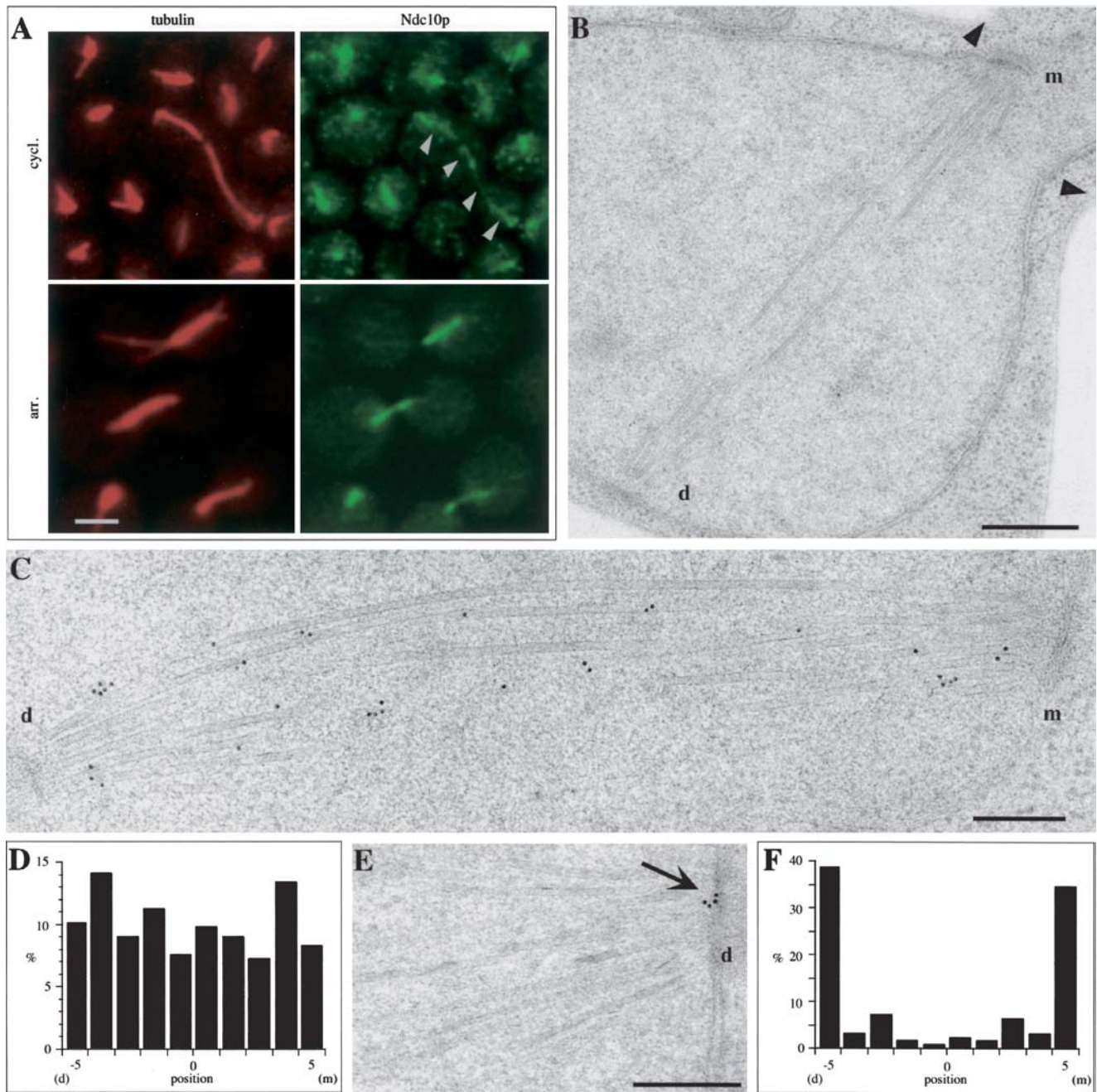
Fig. 4A–F Distribution of Ndc10p in the mitotic spindle of *GALCDC20* cells. **A** Immunofluorescence images of a cycling (*cylc.*) and an arrested (*arr.*) culture. In cycling cultures, Ndc10p is associated with microtubules of short as well as long, anaphase spindles (*white arrowheads*). Arrested *GALCDC20* cells reveal relatively short spindles with an intense Ndc10p signal. **B** Structure of an arrested mitotic spindle, as seen by electron microscopy. Two spindle pole bodies can be distinguished: the "mother" (*m*) and the "daughter" spindle pole body (*d*). The mother spindle pole body is found close to the neck region (*arrowheads*) of the dividing yeast cell. **C** Immunolocalization of Ndc10p in the arrested spindle. **D** Quantitative analysis of the distribution of Ndc10p in the mitotic spindle. The antigen was found to be homogenously distributed. **E** As a control, the distribution of Tub4p (*arrow*) was mapped. **F** This protein was found almost exclusively close to the sites of microtubule attachment (Spang et al.1996). *Bar* represents 250 nm in **A**, **C**, **E**, 500 nm in **B**

The distributions of microtubule plus ends, gold labels, and plus ends with associated gold are shown in Fig. 5C. A three-dimensional model of a spindle of a total length of 0.6 μm (cell no. 2) is shown in Fig. 5D, E. The distributions of microtub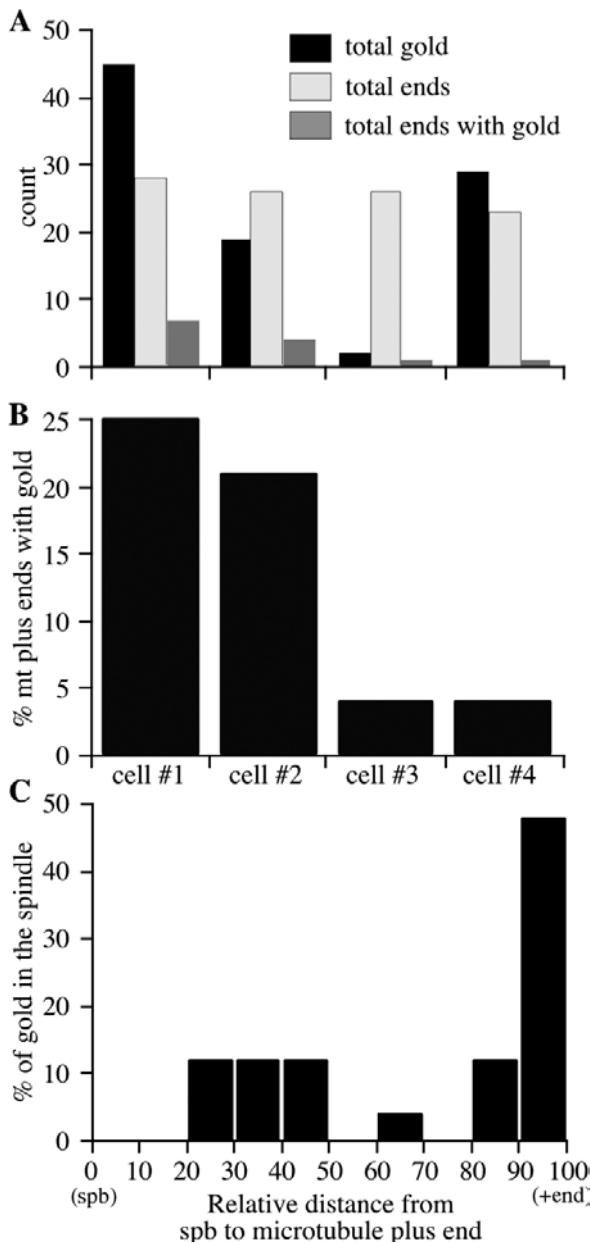ule plus ends, gold labels and gold at microtubule plus ends are given in Fig. 5F. In both models, gold labeling was found associated with microtubule walls as well as with microtubule plus ends. Interestingly, labeling of Ndc10p appears to be more concentrated toward the poles. Quantitative analysis of all

Fig. 5A–F Visualization of Ndc10p in three-dimensional models of wild-type mitotic spindles. **A**, **B** Stereopair of a serial section reconstruction (cell 1). Microtubules originating from the opposite spindle pole bodies are displayed in *red and green*. Interdigitating microtubules are shown in *blue*. Microtubule plus ends are marked with *blue dots*, immunolabeling of Ndc10p is shown by *yellow dots*, and association of plus ends with gold is indicated by *pink dots*. Total length of the spindle is 1.2 μm. **C** Distribution of microtubule plus ends, gold labels, and plus ends with gold labels. **D**, **E** Three-dimensional model of a spindle of total length 0.6 μm (cell 2). **F** Distribution of microtubule plus ends, gold labels, and gold labels at microtubule plus ends. These data suggest lateral as well as terminal association of Ndc10p with microtubules. Some labeling is also found spread within the nucleus (i.e. not bound to microtubules), reflecting endogenous Ndc10p. *Bar* represents 100 nm in **C**, **F**
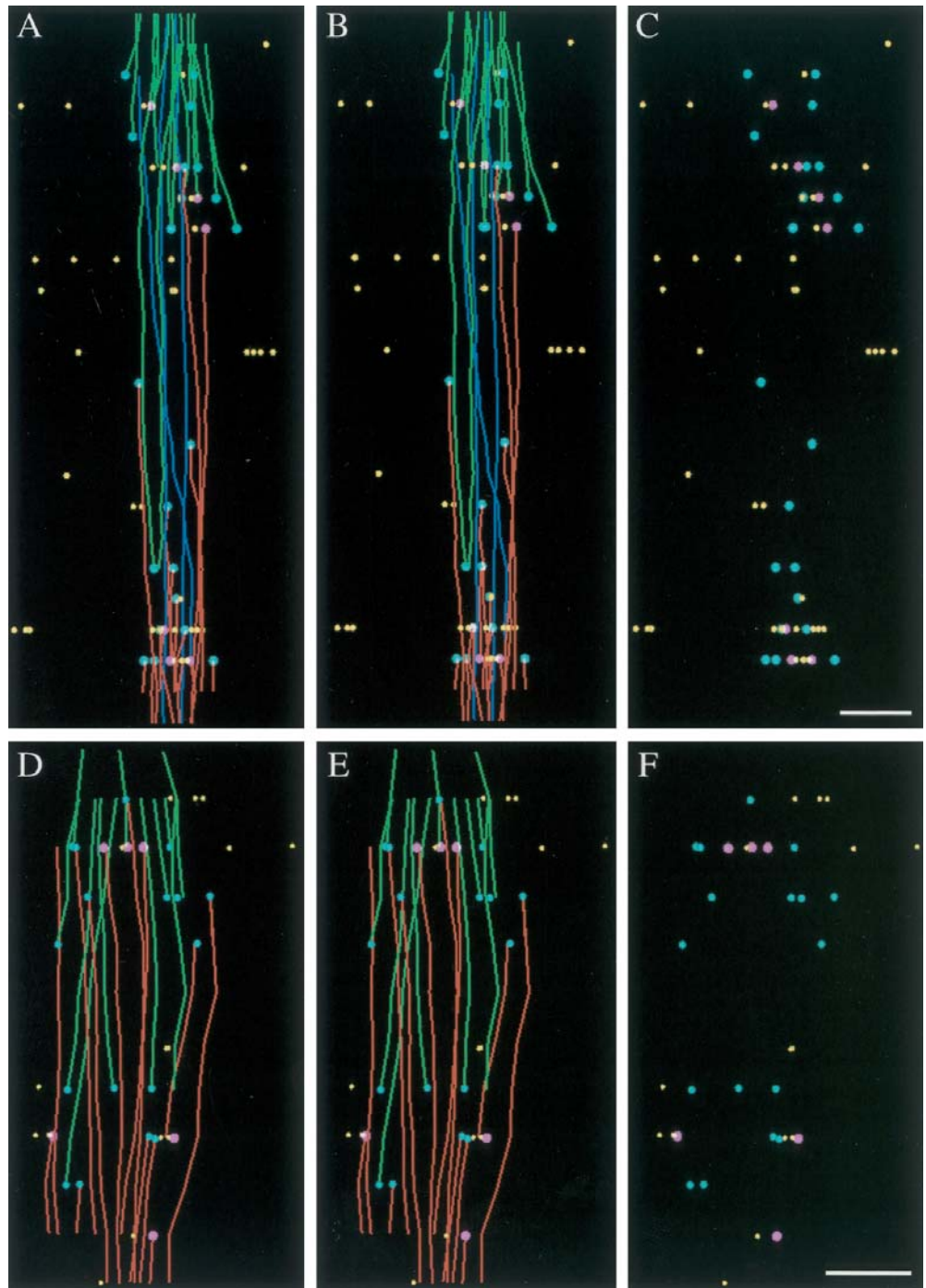
three-dimensional models is given in Fig. 6A. The total number of microtubules appears to be constant in all four models. However, the total number of gold particles detected is variable owing to the difference in spindle length and the on-section labeling technique (i.e., the inability to detect antigens hidden in the section). The percentage of microtubule plus ends with gold labels is given in Fig. 6B. Between 5% and 25% of microtubule plus ends were found associated with gold labels. We also looked at the gold label distributed within the spindle (Fig. 6C). For each gold particle detected, we determined the relative position on individual microtubules. Analyzing the serial section data of cell no. 1, we found roughly 50% of Ndc10p attached to microtubule walls and 50% of the signal attached to microtubule plus ends at metaphase. As a result, serial section reconstruction confirmed the analysis of short and long wild-type spindles in longitudinal sections. Both methods revealed that Ndc10p associates with microtubules laterally as well as terminally.

localize another kinetochore-asociated protein in the budding yeast nucleus. We choose Ndc80p because this protein is not a component of the CBF3 complex. Ndc80p does not bind centromeric DNA, but it is in a complex that is thought to function at the "periphery" of centromeres close to the microtubules (Wigge et al. 1998; Wigge and Kilmartin 2001). In addition, kinetochore binding of Ndc80p is dependent on Ndc10p (Janke et al. 2001). Using a previously described antibody against Ndc80p (Wigge et al. 1998), we performed immunofluorescence on wild-type cells. Immunolabeling of tubulin and Ndc80p is shown in Fig. 7A, B, respectively. The signal is stronger at the poles but nevertheless present as a faint bar along the spindle. This labeling pattern is quite similar to the staining pattern obtained for Ndc10p. To confirm this result, we applied immunoelectron microscopy: Fig. 7C shows labeling of a wild-type metaphase spindle. Again, the pattern obtained matches that of spindle protein distribution with gold label homogeneously distributed throughout the length of the spindle. Thus, apart from its kinetochore function, Ndc80p is non-centromerically distributed in the mitotic spindle. This supports the idea that at least a subset of kinetochore-associated proteins is dispersed throughout the mitotic spindle.

Discussion

The purpose of this study was to analyze the distribution of the kinetochore protein Ndc10p in the *S. cerevisiae* nucleus by immunoelectron microscopy. We have presented evidence that this kinetochore component displays a non-centromeric localization pattern in the mitotic spindle. Three-dimensional analysis showed that Ndc10p was associated with spindle microtubules terminally as well as laterally. Here, we discuss the problems involved in labeling kinetochores in budding yeast, the labeling pattern of Ndc10p relative to other kinetochore components, and finally the possible functions of this non-centromeric distribution.

Fig. 6A–C Quantitative analysis of the serial section reconstructions. Four three-dimensional models were analyzed quantitatively. **A** Total numbers of ends, gold labels, and microtubule ends with gold labels. The models show heterogeneity in the number of colloidal gold particles detected in short spindles. **B** Percentage of microtubule plus ends associated with gold labels. Between 5% and 25% of the labeling was found at microtubule termini. **C** Estimation of the percentage of gold in the spindle associated with microtubule plus ends (cell 1). For each gold particle, the relative position on individual microtubules was determined. The distribution plot shows that 50% of the signal is associated with microtubule walls and 50% with microtubule plus ends

Another kinetochore protein, Ndc80p, is also distributed along spindle microtubules

In order to determine whether the pattern of immunolabeling obtained was unique to Ndc10p, we decided to

Strategies to localize kinetochores in *S. cerevisiae*

Although a number of genetic, biochemical, and in vitro assays have been used to investigate kinetochore function in *S. cerevisiae*, little is known about the precise localization of kinetochores during mitosis. This lack of information is mainly due to the fact that chromosomes are not visible even in electron micrographs of dividing budding yeast cells (Peterson and Ris 1976; Winey et al. 1995). Therefore, to localize kinetochores in budding yeast it is necessary to use an indirect method (i.e., immunoelectron microscopy). In principle, this method allows the distribution of specific kinetochore components in the spindle apparatus to be analyzed. Both pre-embedding and post-embedding labeling can be used for immunoelectron microscopy. In pre-embedding labeling, the efficiency of immunodetection is

425
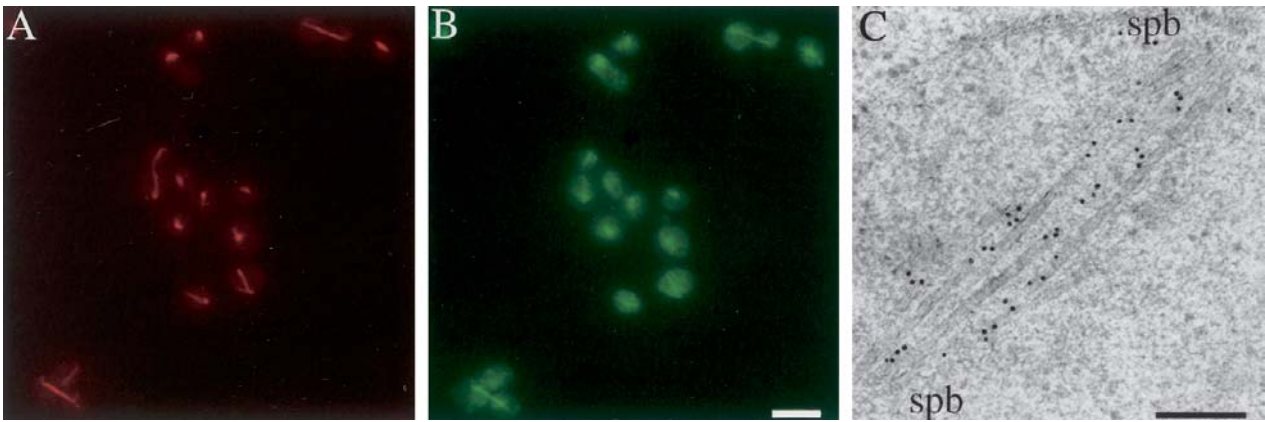
Fig. 7A–C Localization of the kinetochore protein Ndc80p. **A** Immunofluorescence image showing tubulin in wild-type cells. **B** Immunolabeling of Ndc80p. **C** Immunogold labeling of Ndc80p in a wild-type metaphase spindle (*spb* spindle pole body). With both light and electron microscopy, the whole length of the mitotic spindles is decorated with Ndc80p. *Bar* represents 5 µm in **A**, 100 nm in **C**

usually quite high, because the antigens are relatively accessible by primary antibodies. A caveat is that structural preservation in pre-embedding labeling is not optimal because microtubules may partially depolymerize during chemical fixation. Because we wanted to determine whether kinetochore components associate with microtubules terminally or laterally, we considered that this method was limited due to the structural artefacts that it might generate. With post-embedding labeling, optimal structural preservation can be achieved by using fast freezing technology. Therefore, we applied high pressure freezing in combination with freeze substitution (McDonald and Müller-Reichert 2002). This combination of methods has been shown to cryoimmobilize dynamic structures like spindle microtubules within milliseconds and to retain the antigenicity of target proteins (Winey et al. 1995; Zeng et al. 1999). A disadvantage of this method is that the efficiency of labeling is lower than with pre-embedding labeling. Only antigens exposed on the surface of the plastic sections are accessible for immunolocalization, hence antigens present in low copy numbers are extremely hard to detect. As an example, we tried to localize GFP-tagged Mtw1p and Cse4p on thin sections. However, due to the low copy number we were not able to obtain a reproducible staining pattern. Because the architecture of the spindle is preserved well by high pressure freezing, we decided to model labeled spindle microtubules by serial-section reconstruction. Using such a combination of cryotechniques, immunocytochemistry and computer modeling, we were able to generate, for the first time, three-dimensional models of the distribution of a kinetochore component in *S. cerevisiae*.

Localization patterns of kinetochore components

Biochemistry, bandshift analysis and chromatin-dependent immunoprecipitation have conclusively demonstrated that Ndc10p is a centromere-associated protein (Goh and Kilmartin 1993; Sorger et al. 1994; Sassoon et al. 1999). Is this localization pattern found by electron microscopy? "Authentic" kinetochore proteins are expected to be positioned away from the spindle pole bodies in metaphase, but clustered near the spindle pole bodies in anaphase or telophase (Guacci et al. 1994). In contrast to these expectations, we detected Ndc10p throughout the length of microtubules in metaphase spindles as well as fully elongated anaphase spindles by immunoelectron microscopy (Figs. 2, 3, 4). Interestingly, when the distributions of Mtw1p and Ndc10p in the mitotic spindle were compared by light microscopy, a difference in the localization patterns was observed. In contrast to Ndc10p-GFP, no additional localization of Mtw1p-CFP was revealed along the spindle in anaphase (Goshima and Yanagida 2000). This indicated that the kinetochore component Ndc10p, unlike other kinetochore components, might be associated with spindle microtubules in a centromere-independent manner. Interestingly, we showed that such a staining pattern along microtubules in anaphase is not unique to Ndc10p. We obtained similar results for Ndc80p, a protein involved in the formation of the three-dimensional structure of the kinetochore complex. Our results are in agreement with published observations obtained by light microscopy (Wigge et al.1998).

We have shown that Ndc10p is bound to microtubules that originate from the old as well as from the new spindle pole body, shortly before the early mitotic spindle assembles (Fig. 2). Spindle pole bodies duplicate during S-phase when sister kinetochores are thought to attach to microtubule arrays from both poles. It is thought that the Ipl1p/Sli15p complex promotes the turnover of this connection (Tanaka et al. 2002). Our data may provide a visualization of this "preparation" for bipolar attachment that takes place very early on in the cell cycle. Moreover, in short spindles, the localization of kinetochore antigens indicates that a fraction of Ndc10p is localized to microtubule ends, presumably reflecting "true" kineto-

chore labeling, as well as labeling to microtubule walls (Fig. 5). A similar situation also prevails with fully expanded anaphase spindles (Fig. 3), consistent with the observations by light microscopy (Goh and Kilmartin 1993; Zeng et al. 1999; Goshima and Yanagida 2000). Quantification of Ndc10p labels in reconstructions of short mitotic spindles showed that about 50% of the gold was associated with the tips of kinetochore microtubules while another 50% was laterally bound to the walls of the spindle microtubules (Fig. 6). Because tension has to be exerted by microtubules attached to opposite spindle pole, one would expect a centromere protein like Ndc10p to be localized to microtubule plus ends as shown in fission yeast by electron microscopy (Ding et al. 1993). In mammalian cells, kinetochores attach to microtubule walls first and then typically take up a position at the microtubule plus ends (Rieder and Alexander 1990; Skibbens et al. 1993). Such initial lateral binding could possibly contribute to the localization pattern described in S-phase, but not to the staining pattern described in anaphase. In *S. cerevisiae* we do not know the relationship between centromere localization and microtubule plus ends. Possibly, localization of Ndc10p and other kinetochore components throughout the length of the spindle apparatus could represent the distribution of chromosomes over the spindle. A metaphase plate has not been described in *S. cerevisiae* (Winey et al. 1995), rather, chromosomes move back and forth on the spindle (Straight et al. 1997). It is important to note that a number of chromosome and centromere proteins in mammalian cells are left behind at the spindle midzone at anaphase, a phenomenon with largely unknown function (Cooke et al. 1987; Pankov et al. 1990; Andreassen et al. 1991; Yen et al. 1992). Similarly in *S. cerevisiae*, Slk19p is localized both at centromeres and at the anaphase midzone (Zeng et al. 1999). We cannot exclude the possibility that localization at the midzone in late anaphase represents the movement of proteins from kinetochores to the spindle midzone.

Possible functions of non-centromeric distributions of kinetochore components

What is the function of a non-centromeric distribution of a kinetochore component? We suggest that some kinetochore proteins might also be required for aspects of spindle structure. As an example, Dam1p, a component of the Duo1p/Dam1p complex, has been described as the first non-motor microtubule-associated protein involved in mediating kinetochore-spindle attachments (Cheeseman et al. 2001b). Although not required for the assembly of bipolar spindles, Dam1p is required to maintain metaphase and anaphase spindle integrity. Electron microscopy of *dam1* mutants has revealed a variety of diverse structural defects including splayed, bent and broken spindles. In this context, it is interesting to note that *ndc10-1* cells do not sense the spindle checkpoint represented by the Mad1/Mad2 pathway (Tavormina and Burke 1998; Sassoon et al. 1999). Most of these kinetochore studies rely on loss-of-function mutants in these proteins and have not demonstrated that localization of these proteins to kinetochores is required for their checkpoint function. Non-kinetochore dependent distributions of these proteins could possibly be involved in signaling correct spindle assembly. It is also possible that this centromere-independent labeling reflects some kind of turnover (i.e., a movement of Ndc10p along spindle microtubules from the spindle pole body to the microtubule plus end). The localization pattern described in this study would then correspond to attachment sites for kinetochore proteins on spindle microtubules. Alternatively, Ndc10p may well be expressed at levels higher than those restricted to fully functional kinetochores alone (hence the background we always see within the nucleus). In such a case, a pool of excess protein, possibly in an immature state, would be distributed over the whole spindle with a spindle-protein pattern as shown here. However, further studies and more advanced labeling techniques are still required to enable complete understanding of kinetochore turnover in budding yeast.

References

Adams IR, Kilmartin JV. (2000) Spindle pole body duplication: a model for centrosome duplication? Trends Cell Biol 10:329–335

Andreassen PR, Palmer DK, Wener MH, Margolis RL (1991) Telophase disc: a new mammalian mitotic organelle that bisects telophase cells with a possible function in cytokinesis. J Cell Sci 99:523–534

Cheeseman IM, Brew C, Wolyniak M, Desai A, Anderson S, Muster N, Yates JR, Huffaker TC, Drubin DG, Barnes G (2001a) Implication of a novel multiprotein Dam1p complex in outer kinetochore function. J Cell Biol 155:1137–1145

Cheeseman IM, Enquist-Newman M, Müller-Reichert T, Drubin DG, Barnes G (2001b) Mitotic spindle integrity and kinetochore function linked by the Duo1p/Dam1p complex. J Cell Biol 152:197–212

Cheeseman IM, Drubin DG, Barnes G (2002) Simple centromere, complex kinetochore: linking spindle microtubules and centromeric DNA in budding yeast. J Cell Biol 157:1999–2003

Cooke CA, Heck MMS, Earnshaw WC (1987) The inner centromere protein (INCENP) antigens: movement from inner centromere to midbody during mitosis. J Cell Biol 105:2053–2067

Ding R, McDonald KL, McIntosh JR (1993) Three-dimensional reconstruction and analysis of mitotic spindles from the yeast, *Schizosaccharomyces pombe*. J Cell Biol 120:141–151

Fitzgerald-Hayes M, Clarke L, Carbon J (1982) Nucleotide sequence comparisons and functional analysis of yeast centromere DNAs. Cell 29:235–244

Goh PY, Kilmartin JV (1993) NDC10: a gene involved in chromosome segregation in *Saccharomyces cerevisiae*. J Cell Biol 121:503–512

Goshima G, Yanagida M (2000) Establishing biorientation occurs with precocious separation of sister kinetochores, but not the arms, in the early spindle of budding yeast. Cell 100:619–633

Guacci V, Hogan E, Koshland D (1994) Chromosome condensation and sister chromatid pairing in budding yeast. J Cell Biol 125:517–530

He H, Asthana S, Sorger PK (2000) Transient sister chromatid separation and elastic deformation of chromosomes during mitosis in budding yeast. Cell 101:763–775

He H, Rines DR, Espelin C W, Sorger PK.(2001) Molecular analysis of kinetochore-microtubule attachment in budding yeast. Cell 106:195–206

Hoyt MA, He L, Loo KK, Saunders WS (1992) Two *Saccharomyces cerevisiae* kinesin-related gene-products required for mitotic spindle assembly. J Cell Biol 118:109–120

Hyman AA, Sorger PK (1995) Structure and function of kinetochores in budding yeast. Annu Rev Cell Dev Biol 11:471–495

Ito H, Fukuda Y, Murat K, Kimura A (1983) Transformation of intact yeast cells treated with alkali cations. J Bacteriol 153:163–168

Janke C, Ortiz J, Lechner J, Shevchenko A, Shevchenko A, Magiera MM, Schramm C, Schiebel E (2001) The budding yeast proteins Spc24p and Spc25p interact with Ndc80p and Nuf2p at the kinetochore and are important for kinetochore clustering and checkpoint control. EMBO J 20:777–791

Janke C, Ortiz J, Tanaka TU, Lechner J, Schiebel E (2002) Four new subunits of the Dam1-Duo1 complex reveal novel functions in sister kinetochore biorientation. EMBO J 21:181–193

Jiang W, Lechner J, Carbon J (1993) Isolation and characterization of a gene (CBF2) specifying a protein component of the budding yeast kinetochore. J Cell Biol 121:513–519

Lechner J, Carbon J (1991) A 240 kD multisubunit protein complex, CBF3, is a major component of the budding yeast centromere. Cell 64:717–725

Lim HH, Goh PY, Surana U (1998) Cdc20 is essential for the cyclosome-mediated proteolysis of both Pds1 and Clb2 during M phase in budding yeast. Curr Biol 8:231–234

McDonald K, Müller-Reichert T (2002) Cryomethods for thin section electron microscopy. Methods Enzymol 351:96–123

McDonald KL, Mastronarde DN, O'Toole ET, Din R, McIntosh JR (1991) Computer-based tools for morphometric analysis of mitotic spindles and other microtubule systems. EMSA Bull 21:47–53

Measday V, Hailey DW, Pot I, Givan S, Hyland KM, Gagney G, Fields S, Davis TN, Hieter P (2002) Ctf3p, the Mis6 budding yeast homolog, interacts with Mcm22p and Mcm16p at the yeast outer kinetochore. Genes Dev 16:101–113

Müller-Reichert T, Ashford A, Antony C, Hyman A (2000) Ultrastructural localization of antigens in the mitotic spindle of budding yeast using high pressure freezing and freeze substitution. Microsc Microanal 6 (Suppl 2):300–301

Nasmyth K (2002) Segregating sister genomes: the molecular biology of chromosome separation. Science 297:559–565

O'Toole ET, Mastronarde DN, Giddings TH, Winey M, Burke DJ, McIntosh RJ (1997) Three-dimensional analysis and ultrastructural design of mitotic spindles from the cdc20 mutant of *Saccharomyces cerevisiae*. Mol Biol Cell 8:1–11

Ortiz J, Stemmann O, Rank S, Lechner J (1999) A putative protein complex consisting of Ctf19, Mcm21, and Okp1 represents a missing link in the budding yeast kinetochore. Genes Dev 13:1140–1155

Pankov R, Lemieux M, Hancock R (1990) An antigen located in the kinetochore region in metaphase, and on polar microtubule ends in the midbody region in anaphase, characterized using a monoclonal antibody. Chromosoma 99:95–101

Pereira G, Tanaka TU, Nasmyth K, Schiebel E (2001) Mode of spindle pole body inheritance and segregation of the Bfa1p-Bub2p checkpoint protein complex. EMBO J 20:6359–6370

Peterson JB, Ris H (1976) Electron-microscopic study of the spindle and chromosome movement in the yeast *Saccharomyces cerevisiae*. J Cell Sci 22:219–242

Pringle JR, Adams AEM, Drubin DG, Haarer BK (1991) Immunofluorescence methods for yeast. Methods Enzymol 194:565–602

Quan-wen J, Fuchs J, Loidl J (2000) Centromere clustering is a major determinant of yeast interphase nuclear organization. J Cell Sci 113:1903–1912

Rieder CL, Alexander SP (1990) Kinetochores are transported poleward along a single astral microtubule during chromosome attachment to the spindle in newt lung cells. J Cell Biol 110:81–95

Roos U-P (1973) Light and electron microscopy of rat kangaroo cells in mitosis: II. Kinetochore structure and function. Chromosoma 41:195–220

Rose MD, Winston F, Hieter P (1990) Methods in yeast genetics. Cold Spring Harbor Laboratory Press, Cold Spring Harbor, NY

Sambrook J, Fritsch EF, Maniatis T (1989) Molecular cloning: a laboratory manual. Cold Spring Harbor Laboratory Press, Cold Spring Harbor, NY

Sassoon I, Severin FF Andrews PD, Taba MR, Kaplan KB, Ashford AJ, Stark MJ, Sorger PK, Hyman AA (1999) Regulation of *Saccharomyces cerevisiae* kinetochores by the type 1 phosphatase Glc7p. Genes Dev 13:545–555

Schertha H, Loidl J, Schuster T, Schweizer D (1992) Meiotic chromosome condensation and pairing in *Saccharomyces cerevisiae* studied by chromosome painting. Chromosoma 101:590–595

Skibbens RV, Skeen VP, Salmon ED (1993) Directional instability of kinetochore motility during chromosome congression and segregation in mitotic newt lung cells: a push-pull mechanism. J Cell Biol 122:859–875

Sorger PK, Severin FF, Hyman AA (1994) Factors required for the binding of reassembled yeast kinetochores to microtubules in vitro. J Cell Biol 127:995–1008

Sorger PK, Doheny KF, Hieter P, Kopski KM, Huffaker TC, Hyman AA (1995) Two genes required for the binding of an essential *Saccharomyces cerevisiae* kinetochore complex to DNA. Proc Natl Acad Sci U S A 92:12026–12030

Spang A, Geissler S, Grein K, Schiebel E (1996) γ-Tubulin-like Tub4p of *Saccharomyces cerevisiae* is associated with the spindle pole body substructures that organize microtubules and is required for mitotic spindle formation. J Cell Biol 134:429–441

Straight AF, Marshall WF, Sedat JW, Murray AW (1997) Mitosis in living budding yeast: anaphase A but no metaphase plate. Science 277:574–578

Tanaka TU, Rachidi N, Janke C, Pereira G, Galova M, Schiebel E, Stark MJ, Nasmyth K (2002) Evidence that the Ipl1-Sli15 (Aurora kinase-INCENP) complex promotes chromosome biorientation by altering kinetochore-spindle pole connections. Cell 108:317–329

Tavormina PA, Burke DJ (1998) Cell cycle arrest in cdc20 mutants of *Saccharomyces cerevisiae* is independent of Ndc10p and kinetochore function but requires a subset of spindle checkpoint genes. Genetics 148:1701–1713

Wigge PA, Kilmartin JV (2001) The Ndc80p complex from *Saccharomyces cerevisiae* contains conserved centromere components and has a function in chromosome segregation. J Cell Biol 152:349–360

Wigge PA, Jensen ON, Holmes S, Soues S, Mann M, Kilmartin JV (1998) Analysis of the *Saccharomyces* spindle pole by matrix-assisted laser desorption/ionization (MALDI) mass spectrometry. J Cell Biol 141:967–977

Winey M, Mamay CL, O'Toole ET, Mastronarde DN, Giddings TH, McDonald KL, McIntosh JR (1995) Three-dimensional ultrastructural analysis of the *Saccharomyces cerevisiae* mitotic spindle. J Cell Biol 129:1601–1615

Yen TJ, Li G, Schaar BT, Szilak I, Cleveland DW(1992) CEN-P is a putative kinetochore motor that accumulates just before mitosis. Nature 359:536–539

Zeng X, Kahana JA, Silver PA, Morphew MK, McIntosh JR, Fitch IT, Carbon J, Saunders WS (1999) Slk19p is a centromere protein that functions to stabilize mitotic spindles. J Cell Biol 146:415–425